Electronic Supplementary Information (ESI)

Mild Hydrolysis of PET and Electrochemical Energy Recovery via Multifunctional Polyoxometalate Catalysts

Hyeonmyeong Oh[ab], Ye Chan Lee[a], Inhui Lee[ab], Yuri Choi[ab], Jiyeong Kim[ab], Hyeongoo Kim[ab], Kwang Min Kim[ab], Yoonjeong Jo[a], Kwangjin An[bc], Tae Hoon Oh[ac] and Jungki Ryu*[abcd]*

[a]School of Energy and Chemical Engineering, Ulsan National Institute of Science and Technology (UNIST), Ulsan 44919, Republic of Korea

[b]Emergent Hydrogen Technology R&D Center, Ulsan National Institute of Science and Technology (UNIST), Ulsan 44919, Republic of Korea

[c]Graduate School of Carbon Neutrality, Ulsan National Institute of Science and Technology (UNIST), Ulsan 44919, Republic of Korea

[d]Center for Renewable Carbon, Ulsan National Institute of Science and Technology (UNIST), Ulsan 44919, Republic of Korea

*To whom correspondence should be addressed: jryu@unist.ac.kr (J.R.); oh.taehoon@unist.ac.kr (T.H.O.)

Keywords: polyethylene terephthalate, plastic recycling, chemical recycling, electrolysis, fuel cells

EXPERIMENTAL SECTION

Materials

Phosphomolybdic acid ($H_3PMo_{12}O_{40}$, PMA), vanadium oxide (V_2O_5), platinum on carbon (Pt/C), ruthenium (IV) oxide (RuO_2), nitric acid (HNO_3), formic acid (FA), Nafion solution (5 wt% in ethanol), and potassium hydroxide (KOH) were purchased from Sigma-Aldrich (USA). Multi-walled carbon nanotubes (MWCNTs, >95%, outer diameter 5-15 nm) were obtained from US Research Nanomaterials, Inc. (USA). A platinum wire, N,N-dimethylformamide (DMF), glycolic acid (GA), ethylene glycol (EG), and dimethyl sulfoxide (DMSO, <0.025% H_2O) were sourced from Alfa Aesar (USA). Sulfuric acid (>95.0%) was supplied by Junsei Chemical (Japan). Nafion™ 117 membrane was obtained from Fuel Cell Store. Commercial poly(ethylene terephthalate) (PET) bottles were collected from post-consumer Coca-Cola packaging and used as a representative source of plastic waste. According to standard industry specifications for carbonated beverage bottles, the material consists of >99% PET resin (with minor additives) and exhibits an intrinsic viscosity of approximately 0.80–0.84 dL/g, corresponding to a number-average molecular weight (M_n) of approximately 24,000–30,000 g/mol.

PET depolymerization with PMA

To investigate the depolymerization of PET using PMA, two sets of reaction conditions were employed. In the first set, PMA was dissolved in 10 mL of 1 M H_2SO_4 to prepare a 0.5 M solution. Reagent-grade PET pellets (3 mm in diameter) or cryo-milled PET powder (<425 μm) were added (1 g) to the solution in a sealed autoclave. To prepare the cryo-milled PET powder, PET pellets or bottle pieces were first frozen using liquid nitrogen and subsequently pulverized for 15 min at 2000 rpm using an IQ Mill-2070. The resulting powder was then sieved to obtain

a particle size <425 μm (40 mesh). The reaction mixture was then heated at 100 ℃, 150 ℃, or 175 ℃ for various time intervals (1-5 h) to evaluate the effect of temperature on depolymerization efficiency. For the second set of experiments, designed to enable depolymerization under milder conditions (<100 ℃), a 0.5 M PMA solution was prepared by mixing 5 mL of DMSO with 5 mL of 1 M H_2SO_4. In this system, 1 g of cryo-milled PET powder (<425 μm) or pieces of commercial post-consumer PET bottles were reacted with this PMA solution in an autoclave. The mixture was heated at temperatures below 100 ℃ for durations ranging from 1 to 5 h to identify optimal conditions for low temperature depolymerization.

Model reactions for product oxidation

To investigate the oxidative transformation of PET-derived intermediates, model reactions were conducted using EG, GA, and FA as substrates. Each compound was added to a 0.5 M PMA solution in a 1:1 (v/v) mixture of DMSO and 1 M H_2SO_4, at a concentration equivalent to the theoretical yield from 1 g of PET (e.g., 5.2 mmol in 10 mL for EG). The reaction mixtures were heated at 100 ℃ under continuous stirring. Aliquots were collected at predetermined time intervals for analysis by high-performance liquid chromatography (HPLC) to monitor the progression of oxidation and quantify intermediate and final products.

Characterization

Raman spectroscopy was conducted using an alpha 300S confocal Raman microscope (WITec, Germany) equipped with a 532 nm laser to confirm the adsorption of PMA onto PET surfaces. The concentration of reduced PMA species was determined by UV-visible spectroscopy using a V-730 spectrophotometer (JASCO, Japan), with absorbance recorded from 400 to 1100 nm.

Quantification was based on a pre-established calibration curve correlating absorbance with known degrees of PMA reduction. Proton nuclear magnetic resonance (^{1}H NMR) spectroscopy was performed using a 400 MHz Bruker spectrometer to analyze TPA recovered from PET depolymerization and to confirm deuterium incorporation in the labeling experiments. D_2O was used as the solvent for NMR analysis of deuterium-substituted samples. Fourier Transform Infrared (FT-IR) spectroscopy was conducted using a 670/620 Spectrometer (Agilent, USA) to characterize the functional groups present in synthesized BHET and re-polymerized PET (r-PET). The spectra were compared with those of commercial PET and recovered TPA to confirm structural integrity and successful re-polymerization.

Preparation of Deuterium Substituted PMA Solution

To prepare the deuterium-substituted PMA solution, 5 mmol of $H_3[PMo_{12}O_{40}]$ was dissolved in 10 mL of D_2O. The solution was stirred at room temperature for 24 hours to facilitate hydrogen-deuterium exchange. Following the exchange, the D_2O solvent was removed under reduced pressure using a rotary evaporator. The resulting deuterated PMA solution was then used directly in PET depolymerization experiments to investigate the proton transfer mechanism.

Quartz Crystal Microbalance (QCM) Analysis

For adsorption studies, QCM sensors were coated with a thin film of PET. This was achieved by dissolving commercial PET pellets in hexafluoro isopropanol (HFIP) and drop-casting the resulting solution onto the gold electrode surface of the QCM sensor. The coated sensors were first dried under a gentle stream of nitrogen gas and then dried in a vacuum oven at 60 °C to remove any residual solvent. The prepared sensors were then mounted in a QCM flow module

for real-time monitoring. Frequency and dissipation shifts were recorded upon exposure to various solutions, including deionized (DI) water, 1 M H_2SO_4, 0.5 M PMA, and 0.5 M PMA in 1 M H_2SO_4, at room temperature.

Synthesis of Recycled PET (rPET) from Recovered TPA

Recycled PET (rPET) was synthesized from recovered TPA through a two-step catalytic process involving esterification and polycondensation. TPA was first reacted with EG, typically used in excess at a molar ratio of TPA:EG ranging from 1:1.2 to 1:2.0, to produce BHET. The esterification reaction was carried out at 220 °C under atmospheric pressure. The resulting BHET-containing underwent polycondensation at 280 °C under vacuum to yield rPET. Appropriate catalysts were employed for both the esterification and polycondensation steps to facilitate efficient conversion and polymer chain growth.

Preparation of Membrane Electrode Assembly Using Pt/C- or RuO2- Coated Carbon Nanotube Paper (CNTs paper)

To fabricate the membrane electrode assembly (MEA), 100 mg of MWCNTs were dispersed in 100 mL of DMF and ultrasonicated for 1 h to obtain a uniform dispersion. The resulting suspension was vacuum filtered through a polyvinylidene fluoride membrane with a pore size of 0.2 μm to form a free-standing CNT paper. This paper was then dried at 60 ℃ under vacuum for 12 h to remove residual solvent. To prepare catalyst ink, an appropriate amount of catalyst powder—either Pt/C (for hydrogen evolution reactions or fuel cell applications), RuO_2 (for oxygen evolution reactions), or potentially no catalyst (to utilize the intrinsic activity of the CNT paper for PMA/vanadium redox reactions)—was added to 300 μL of a 50:50 (v/v) isopropyl

alcohol-water mixture. The mixture was vigorously shaken and ultrasonicated for 25 min. Nafion solution (5 wt% in ethanol) was then added as a binder, followed by an additional 25 min of ultrasonication. The prepared ink was drop-casted onto the CNT paper at a catalyst loading of 0.32 mg/cm^2 and dried at 60 °C for 1 h. The catalyst-coated CNT papers were then assembled on both sides of a Nafion™ 117 membrane. The complete assembly was hot-pressed at 120 °C and 3 MPa for 5 min to form MEA, which was subsequently used in electrolyzer and fuel cell tests.

Electrochemical Characterization

Electrochemical measurements, including linear sweep voltammetry, cyclic voltammetry, and chronoamperometry, were performed using a WMPG1000 multichannel potentiostat/galvanostat. Basic electrochemical characterizations were conducted in a standard three-electrode configuration consisting of a Pt wire as the counter electrode, a Ag/AgCl reference electrode, and a working electrode immersed in the electrolyte of interest (e.g., 0.5 M PMA in 1 M H_2SO_4, with or without added substrate). For gas analysis, evolved products were collected from the outlet of a custom-built H-cell and analyzed using a GC-2010 Plus gas chromatograph (Shimadzu Corporation, Japan).

Assembly of PEM Electrolyzers and Redox Fuel Cells and Test Methods

The performance measurement of the proton exchange membrane (PEM) electrolyzer and vanadium redox fuel cell was evaluated using a MEA composed of two CNT paper electrodes and a Nafion™ 117 membrane sandwiched between them. Each CNT electrode incorporated a serpentine flow channel on the inner face (2 mm width × 2 mm depth × 5 cm length), resulting

in a total active area of 1 cm^2. For electrolyzer testing, chronoamperometry was conducted with 1 M H_2SO_4 supplied to the cathode and 0.5 M pre-reduced PMA solution—previously reacted with PET—to feed the anode. A constant voltage of 1.2 V was applied across the cell, and the resulting current density was recorded over time. The Faradaic efficiency for hydrogen production was calculated based on the total charge passed and the amount of H_2 quantified via online GC. For fuel cell testing, the catholyte was replaced with a 1 M V_2O_5 solution. To facilitate the reduction of V_2O_5, 1 mL of HNO_3 was added per 100 mL of solution, and a continuous flow of O_2 was maintained. The anode was again fed with the 0.5 M pre-reduced PMA solution. Fuel cell performance was evaluated by monitoring polarization curves and power density output.

Product Analysis with Liquid Chromatography (LC)

HPLC was employed to analyze the liquid-phase products formed during PET depolymerization. The reaction solution containing PMA and depolymerized PET was diluted 100-fold with deionized (DI) water prior to analysis. Chromatograms were obtained using a Waters HPLC system equipped with a 1525 high-pressure binary pump and a 2414 refractive index (RI) detector. An Aminex HPX-87H capillary column (300 mm × 7.8 mm) was used for HPLC analysis. The mobile phase consisted of a 5 mM H_2SO_4 aqueous solution, delivered at a flow rate of 0.6 mL/min. The injection volume was set to 50 μL. EG, GA, and FA were identified and quantified by comparing retention times and peak areas with those of external standards of known concentrations.

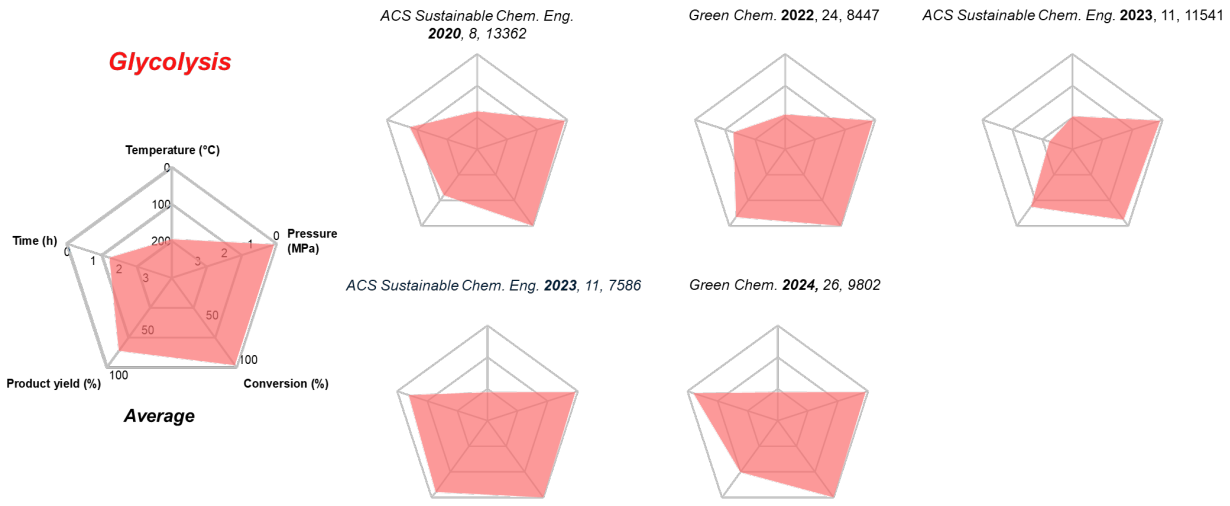

Fig. S1 Comparative radar chart analysis of PET glycolysis systems using key parameters. Radar charts representing five literature-reported PET glycolysis systems and an averaged radar chart calculated from all five systems are presented. Each chart visualizes key parameters—reaction temperature (°C), pressure (MPa), PET conversion (%), BHET (bis(hydroxyethyl) terephthalate) yield (%), and reaction time (h). The average chart highlights the general performance trends of conventional glycolysis methods, which typically require high temperatures and extended reaction times, despite achieving high conversion rates and moderate BHET yields.

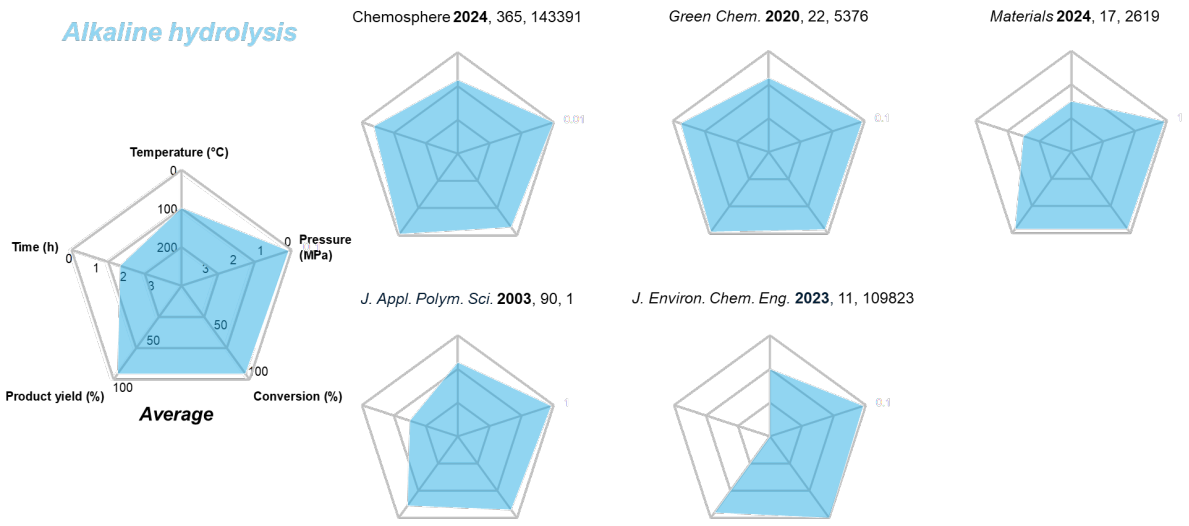

Fig. S2 Comparative radar chart analysis of PET alkaline hydrolysis systems from the literature. Radar charts representing five literature-reported PET alkaline hydrolysis systems and an averaged radar chart calculated from all five systems are presented. Each chart visualizes key parameters—reaction temperature (°C), pressure (MPa), PET conversion (%), TPA yield (%), and reaction time (h). The average performance trend indicates that alkaline hydrolysis generally enables high PET conversion and TPA yield at ambient pressure. However, it often requires high pH and moderately elevated temperatures, which may limit environmental compatibility and downstream processing efficiency.

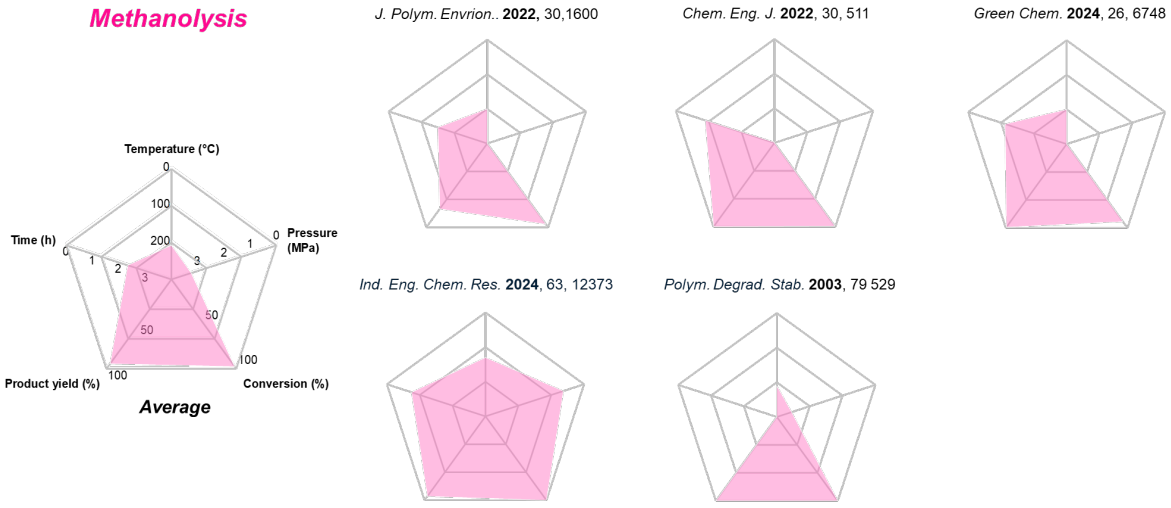

Fig. S3 Comparative radar chart analysis of PET methanolysis systems using key parameters. Radar charts representing five literature-reported PET methanolysis systems and an averaged radar chart calculated from all five systems are presented. Each chart visualizes key parameters—reaction temperature (°C), pressure (MPa), PET conversion (%), DMT (dimethyl terephthalate) yield (%), and reaction time (h). The average chart highlights the typical features of methanolysis systems, which generally achieve high PET conversion and DMT yields but require high temperatures, high pressures, and prolonged reaction durations, thereby increasing process complexity and energy consumption.

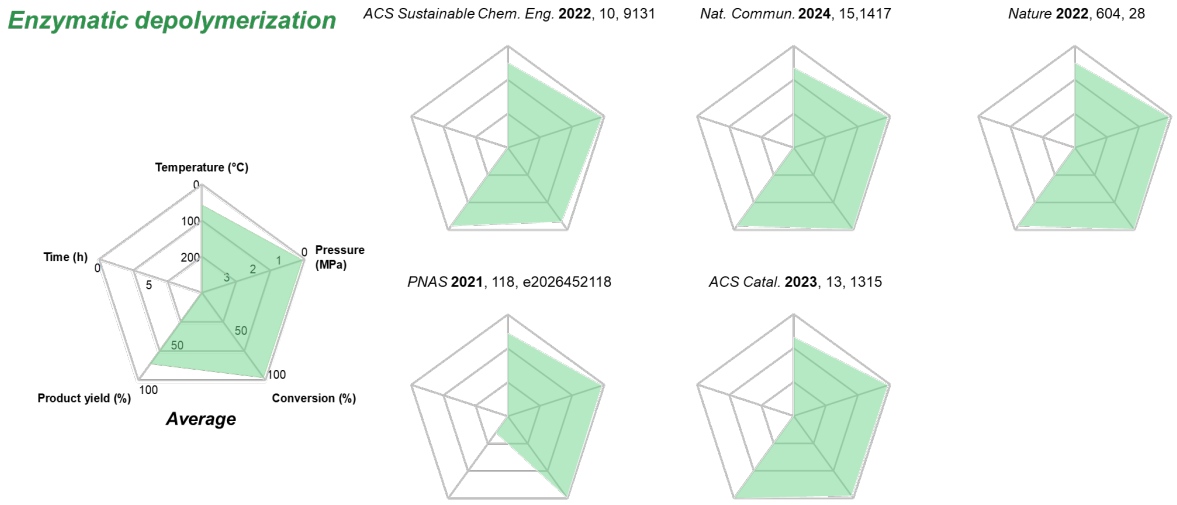

Fig. S4 Comparative radar chart analysis of enzymatic PET depolymerization systems using key parameters. Radar charts representing five literature-reported enzymatic depolymerization systems and an averaged radar chart calculated from all five systems are presented. Each chart visualizes key parameters—reaction temperature (°C), pressure (MPa), PET conversion (%), TPA yield (%), and reaction time (h). The average chart highlights the characteristic features of enzymatic depolymerization systems, which operate under mild temperature and ambient pressure conditions with relatively high product yield but are generally limited by slow reaction rates and enzyme-related constraints, such as stability and activity.

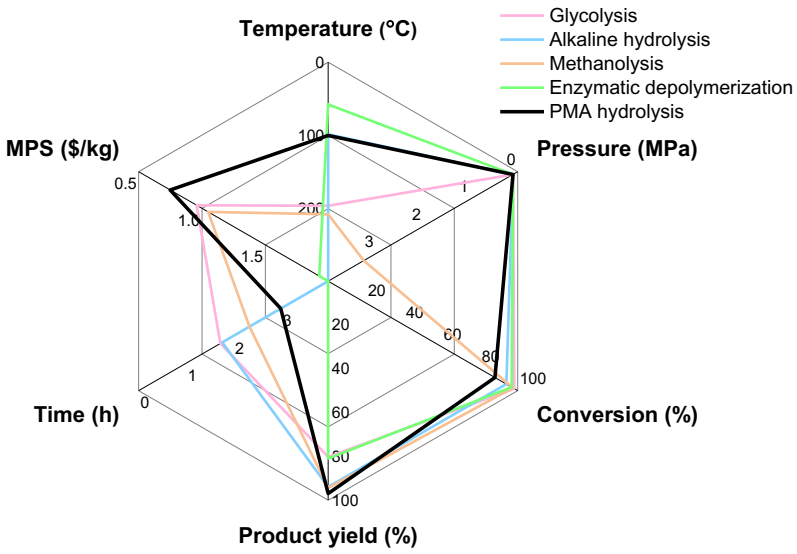

Fig. S5 Comparative performance analysis of PET depolymerization methods including PMA hydrolysis. Radar chart comparing averaged performance of conventional PET depolymerization methods—glycolysis, alkaline hydrolysis, methanolysis, and enzymatic depolymerization—with the PMA-based hydrolysis system developed in this study. Key parameters—reaction temperature (°C), pressure (MPa), PET conversion (%), product yield (%), reaction time (h), and minimum selling price (MSP, $/kg)—are normalized for cross-comparison. The PMA system exhibits a balanced and superior profile, by achieving high PET conversion (~95%), product yield (~97%), and a highly competitive MSP of $0.81/kg, under significantly milder operating conditions (100 °C, ambient pressure) and moderate reaction time (3 h), highlighting its potential as a low-energy, high-efficiency, and most cost-effective alternative for PET chemical recycling.

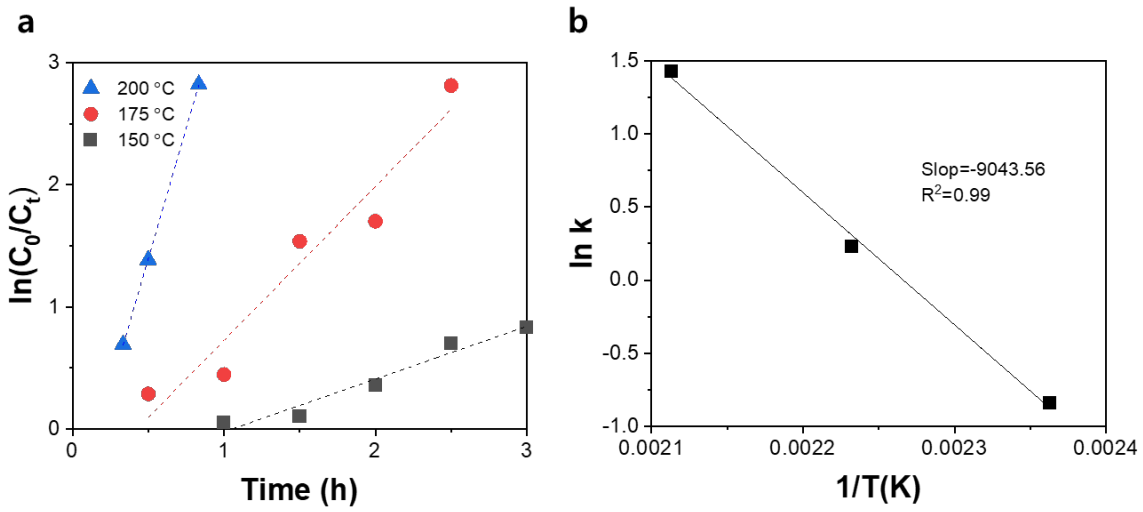

Fig. S6 Activation energy of PET depolymerization using reagent-grade PET pellets without co-solvent. (a) Reaction kinetics of PET depolymerization at 150 °C (black squares), 175 °C (red circles), and 200 °C (blue triangles), plotted as $\ln(C_0/C_t)$ versus time using reagent-grade PET pellets. (b) Arrhenius plot constructed from the rate constants (k) obtained at each temperature in (a), yielding an activation energy of 75.2 kJ/mol for PET depolymerization catalyzed by PMA in aqueous solution.

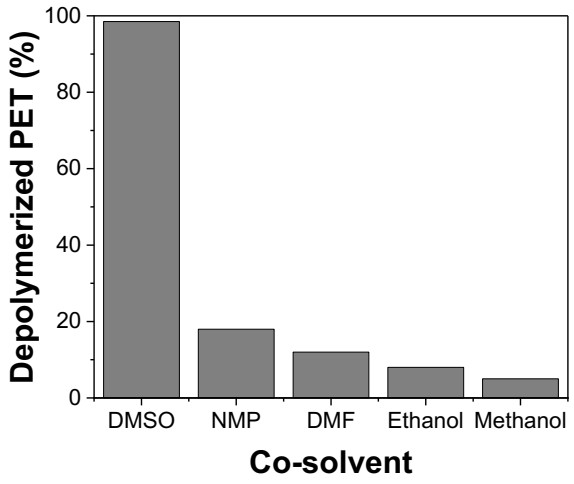

Fig. S7 Comparison of PET depolymerization efficiency using different co-solvents. Reaction conditions: 100 °C, 3 h, 1 M H_2SO_4 with 0.5 M PMA. DMSO exhibited superior performance (>98% conversion), whereas other solvents tested (NMP, DMF, methanol, ethanol) resulted in negligible conversion (<20%).

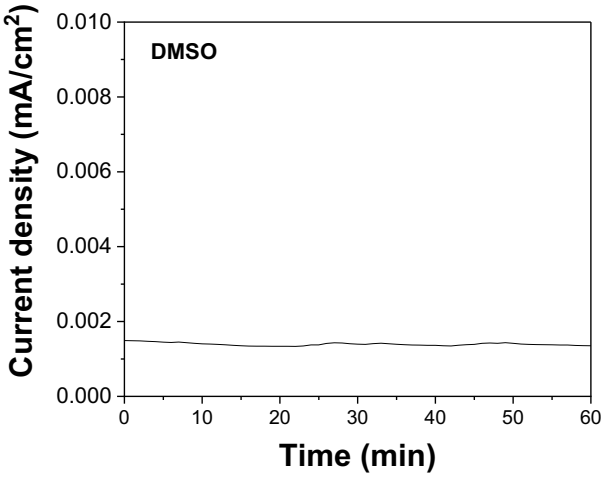

Fig. S8 Electrochemical stability of DMSO. Chronoamperometric response of a 1:1 (v/v) mixture of DMSO and 1 M H_2SO_4 at an applied voltage of 1.2 V *vs.* RHE, recorded over 60 min. The current density remained below 0.002 mA/cm^2, indicating that DMSO is electrochemically stable in oxidative conditions.

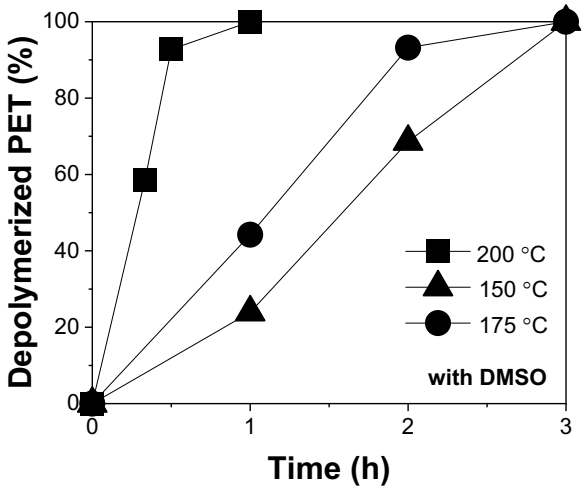

Fig. S9 Temperature-dependent PET depolymerization efficiency in a DMSO–water mixture without cryo-milling. PET depolymerization was conducted using commercial PET bottle pieces at 150, 175, and 200 °C in a 1:1 (v/v) mixture of DMSO and 1 M H_2SO_4 containing 0.5 M PMA. At all temperatures tested, the presence of DMSO enhanced PET depolymerization efficiency compared to the purely aqueous system.

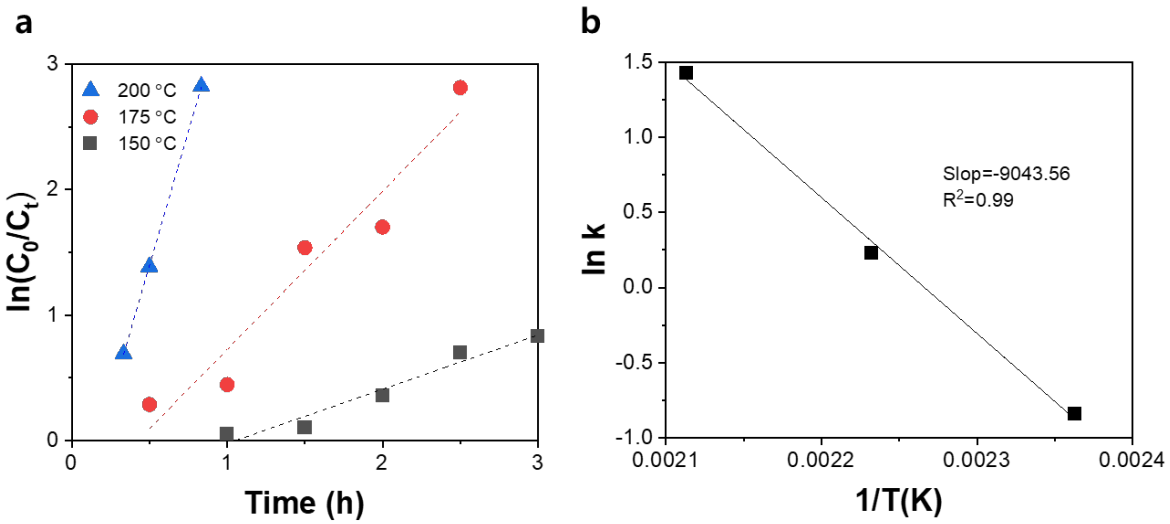

Fig. S10 Kinetic and Arrhenius analysis of PET depolymerization in a DMSO-water mixture. (a) Time-dependent PET depolymerization plotted as ln(C0/Ct) versus time at 150, 175, and 200 °C using a 1:1 (v/v) mixture of DMSO and 1 M H_2SO_4 containing 0.5 M PMA. (b) Arrhenius plot constructed from the rate constants, yielding an apparent activation energy of 70.9–72.9 kJ/mol, which is lower than that observed in aqueous PMA systems.

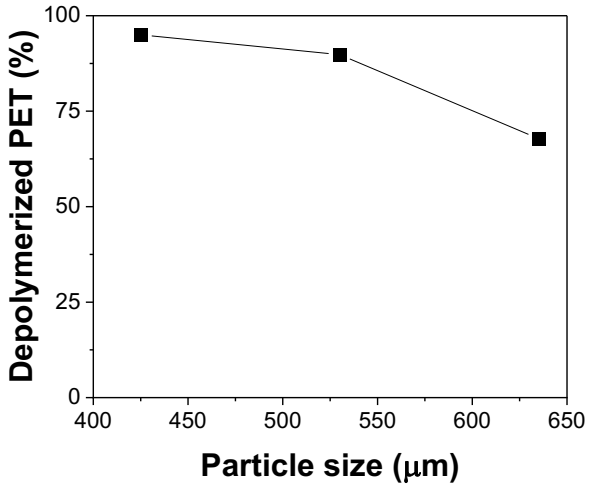

Fig. S11. Effect of PET particle size on depolymerization efficiency. Reactions were conducted at 100 °C in 1 M H_2SO_4/DMSO with 0.5 M PMA using three PET size fractions: small (<425 μm), medium (425–635 μm), and large (635–1000 μm). The higher conversions observed with finer particles highlight the critical role of surface area in governing the depolymerization rate under these mild heterogeneous conditions.

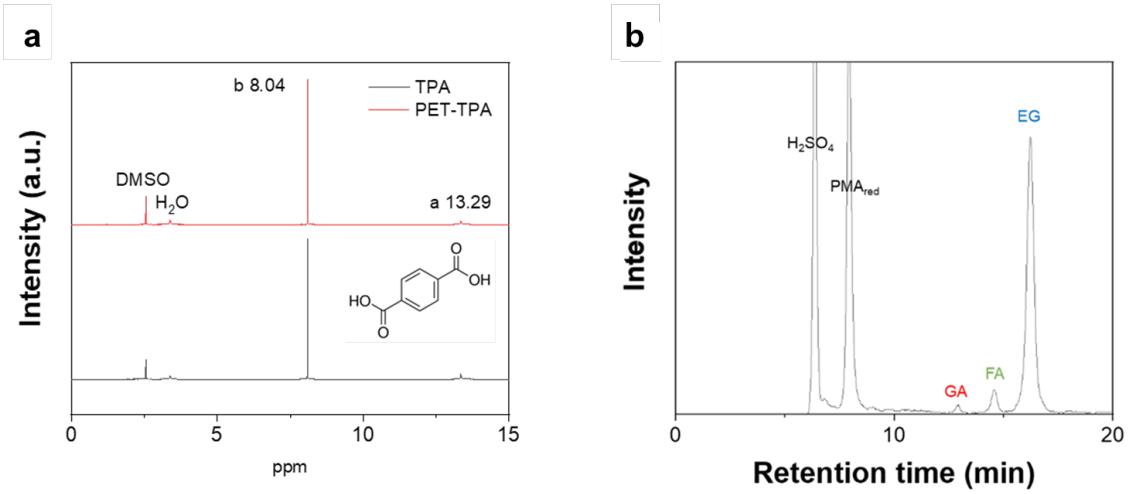

Fig. S12 Analysis of depolymerization products obtained from PMA-catalyzed PET hydrolysis. (a) ^{1}H NMR spectra of commercial TPA and TPA recovered from PET depolymerization using PMA, and (b) HPLC chromatogram of liquid products from the reaction conducted at 100 ℃ for 1 h using 0.5 M PMA in a 1:1 (v/v) mixture of DMSO and 1 M H_2SO_4. The recovered TPA exhibited identical proton signals to commercial TPA. EG, GA, and FA were clearly detected during PET depolymerization.

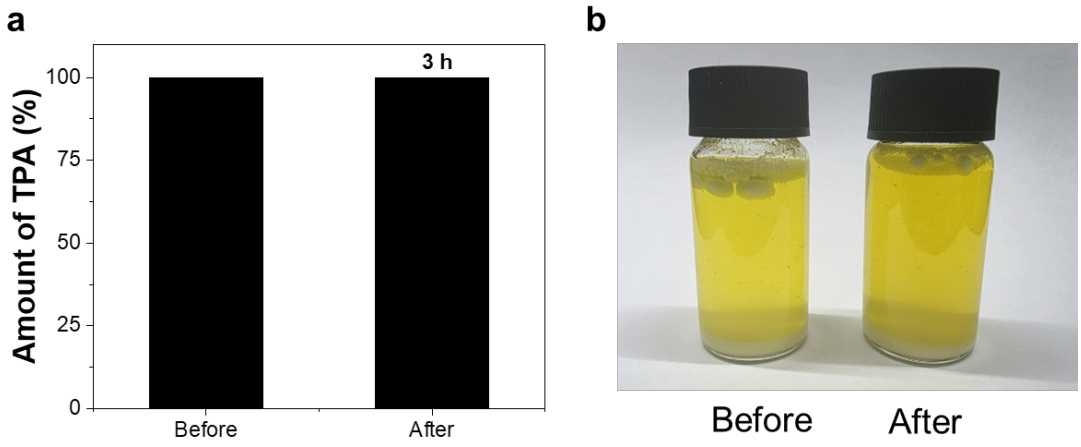

Fig. S13 Experimental validation of TPA stability under PET depolymerization conditions. To evaluate the oxidative stability of TPA in the presence of PMA, (a) the concentration of TPA (86.3 mg/mL)—corresponding to the theoretical yield from the depolymerization of 1 g of PET—was quantified before and after incubation in 0.5 M PMA solution at 100 °C for 3 h, showing no significant change in TPA content. (b) Photographs of the reaction media before and after incubation show that the yellow color of PMA remained in its oxidized state, confirming that TPA did not undergo oxidation under these conditions.

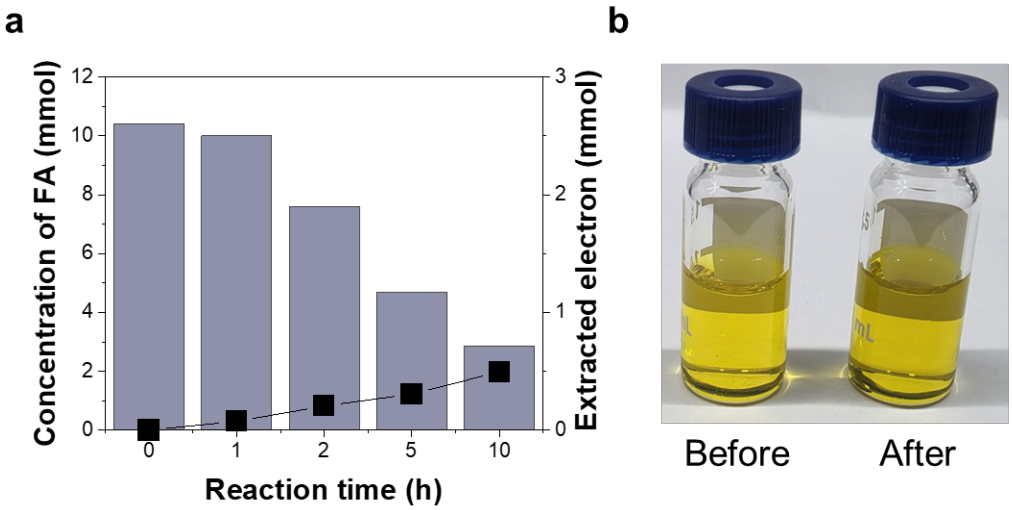

Fig. S14 Limited electron extraction from formic acid (FA) during reaction with PMA. (a) Time profiles of FA concentration and the corresponding number of extracted electrons during its reaction with PMA show that only a small amount of FA was oxidized over time. (b) Digital images of the reaction solution before and after incubation illustrate that the yellow color of PMA remained, indicating negligible redox activity.

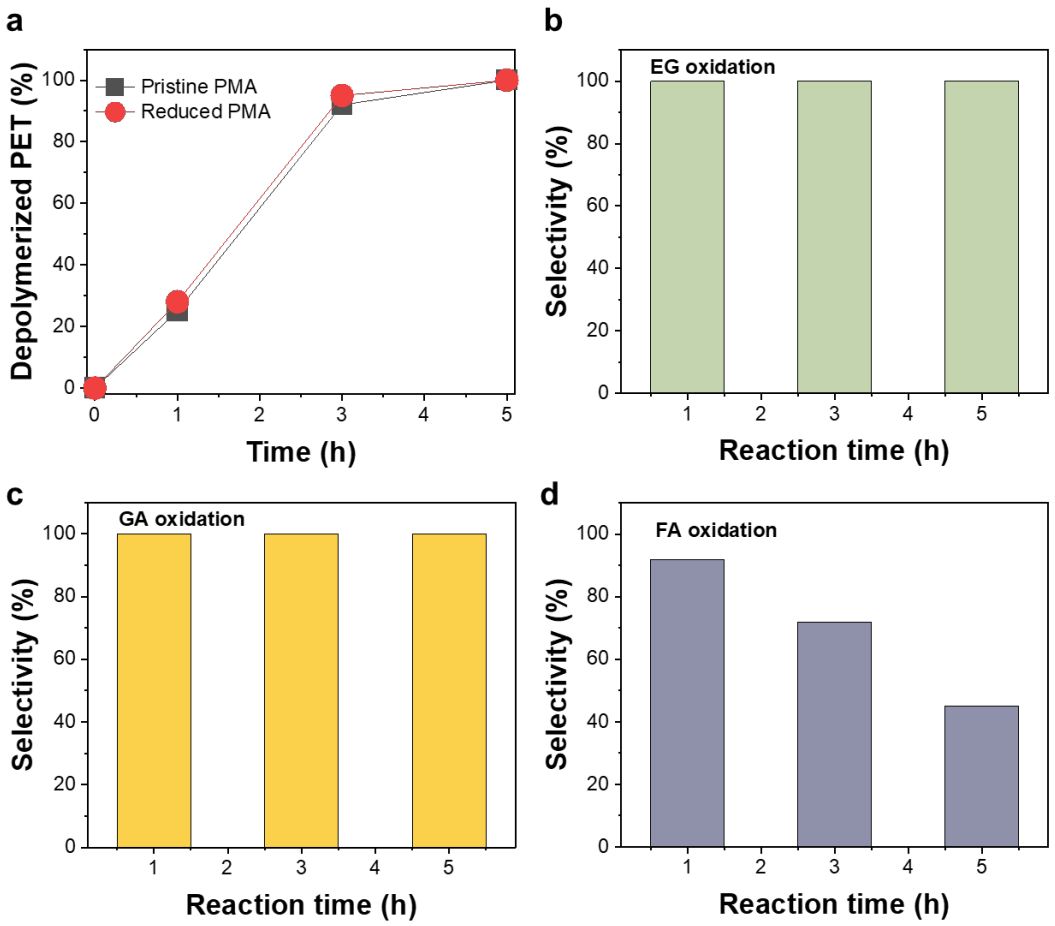

Fig. S15 Inactivity of reduced PMA toward PET-derived intermediates. To examine the role of the PMA redox state in PET oxidation, control experiments were conducted using reduced PMA. (a) PET depolymerization proceeded to a similar extent as with oxidized PMA, indicating that hydrolysis is not affected by the PMA reduction states. However, no electron extraction was observed, suggesting that redox activity is essential for oxidative steps. (b, c) EG and GA remained unreacted in the presence of reduced PMA, confirming the absence of further oxidation. (d) FA underwent decomposition in the presence of reduced PMA, suggesting that its degradation proceeds via acid catalysis.

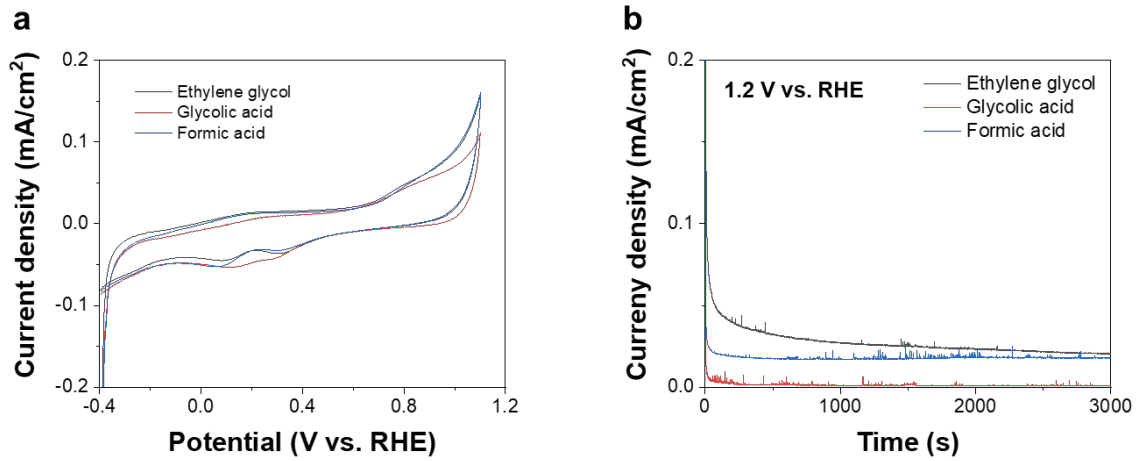

Fig. S16 Electrochemical stability of PET-derived organic intermediates. (a) Cyclic voltammetry (CV) curves of ethylene glycol (EG), glycolic acid (GA), and formic acid (FA) measured in a 1 M H_2SO_4/DMSO electrolyte in the absence of PMA. The initial concentrations of EG, GA, and FA were each 0.52 M, corresponding to the maximum concentration of EG than can be produced from the depolymerization of 1 g PET under the reaction conditions used in this study. (b) Enlarged view of the current density near the operating anodic potential (1.2 V vs. RHE). The negligible current density confirms that these organic species are electrochemically stable and are not oxidized at the anode during the PMA regeneration process.

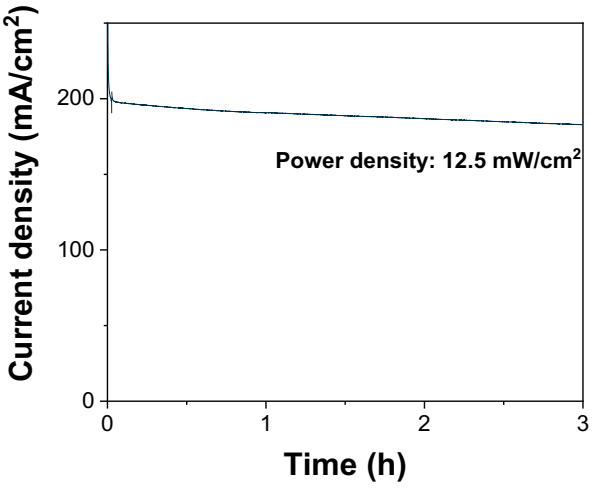

Fig. S17 Continuous operation of the redox fuel cell using reduced PMA. Chronoamperometric measurement of the redox fuel cell over 3 h of operation shows a stable current density with minimal decay, which can be attributed to the consumption of reduced PMA. The system maintained a peak power density of 12.5 mW/cm^2, demonstrating the viability of PMA-mediated electron extraction for energy generation.

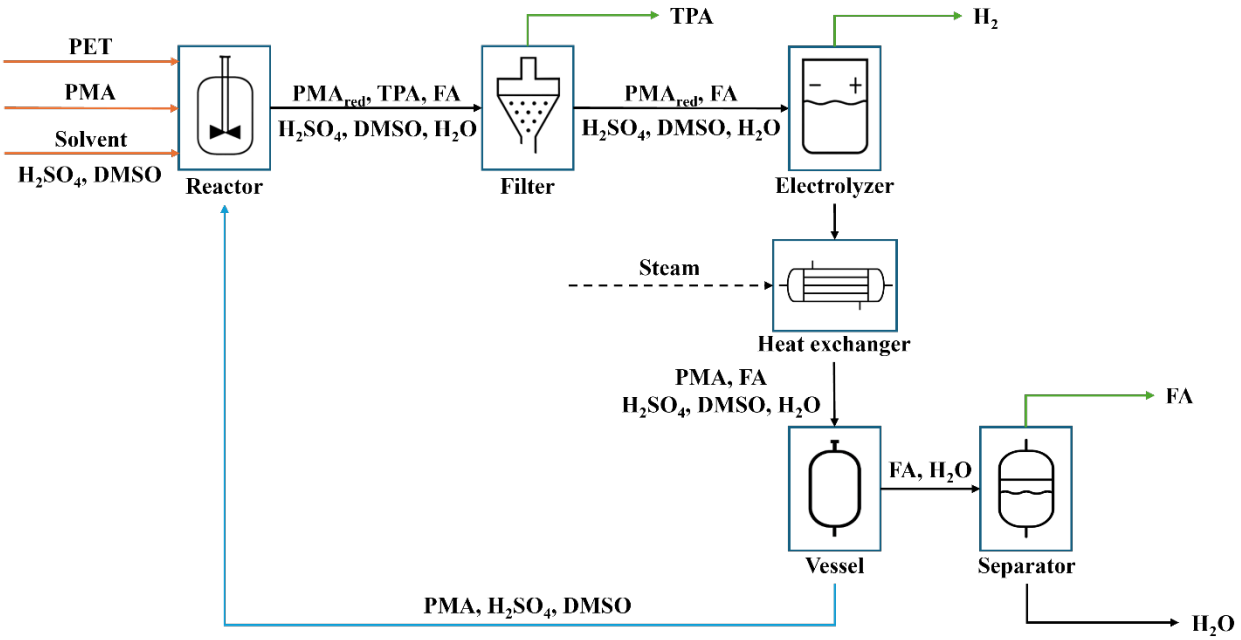

Fig. S18 Block flow diagram of the PMA-catalyzed PET recycling process. A 1:1 v/v mixture of H_2SO_4 and DMSO is used as solvent at a total concentration of 1 M. PET is depolymerized in a batch reactor at 100 °C for 2h, followed by electrochemical regeneration of PMA at 25 °C. Separation is performed at 180 °C to recover and recycle PMA, DMSO, and H_2SO_4. The extraction of FA from water follows the process developed by Laitinen et al.4. Due to the difficulty of separating DMSO from EG, the economic analysis was performed under the condition that it maximizes FA selectivity.

Table S1. Unit prices of materials for feedstock and product.

List	Price($/kg)	Reference
Waste PET	0.1	Echemi trading data
PMA	0.01	Made-in-China[a]
H_2SO_4	0.037	Echemi trading data
Dimethyl Sulfoxide	1.5	Echemi trading data
Terephthalic Acid	0.94	Echemi trading data
Formic Acid	0.72	Echemi trading data
H_2	2—8	-
H_2O	0.00022	1

a. Taken from online trade market. (https://sdyifan.en.made-in-china.com/product/IaqrtlQcvehg/China-High-Quality-Phosphomolybdic-Acid-CAS-No-51429-74-4-Manufacturer.html?pv_id=1iujis7vaefb&faw_id=1iujj07mq052&bv_id=1iujj5tg09a&pbv_id=1iujis7649fd)

Table S2. Unit costs for electrochemical and thermal processes.

List	Price	Unit	Reference
Electrolyzer	10,000	$\$/m^2$	1
Electricity	0.0953	\$/kWh	Kepco data
H_2 Electrolysis Energy	31.9	kWh/kg H_2	-
Mechanical Crushing Electricity	13	\$/ton PET	-
Reactor heating Electricity	17.00	\$/ton PET	2
Cryogenic grinding Electricity	5.72	\$/ton PET	3

Table S3. Financial and operational assumptions for techno-economic analysis.

List	Value	Unit	Reference
Lifetime	30	year	4
Discount rate	10	%	4
Capital recovery factor	0.11	-	-
Capacity Factor	0.8	-	1
CEPCI of 2016	541.7	-	a
CEPCI of 2023	800.8	-	a
Scaling factor	0.6	-	2

Table S4. Summary of techno-economic analysis of PET recycling via PMA hydrolysis at a plant capacity of 35,000-ton PET/year.

Parameter	Value ($ y^{-1})
Capital Cost: PMA Hydrolysis	
Feedstock Pretreatment	2,905,436
PET Depolymerization	2,813,102
TPA Filtration	2,898,827
Catalyst	9,126
Solvent	826,814
Capital cost: Electrolysis	
Electrolyzer	2,516,275
H_2 Storage	162,167
Capital Cost: Distillation	
FA Distillation	1,255,389
OSBL (Outside Battery Limits Capital)	2,823,952
Total Capital Cost	**16,211,088**
Operational Cost	
Feedstock	2,122,762
Make-up (Catalyst)	31,978
Make-up (Solvent)	2,897,158
Utility	21,278,166
Maintenance	3,630,317
Operation	3,630,317
Total Operational Cost	**33,590,699**
Total Annual Cost	**49,801,786**
Product	
TPA	28,454,002
FA	10,219,279
H_2	14,919,303
Revenue	**53,592,584**
Profit	**3,790,798**

1. Annualized Capital Cost

The annual capital cost represents the yearly recovery of the total CAPEX over the project lifetime. It was calculated as follows:

$$\text{Annualized capital cost} = \sum \text{CAPEX} \times \text{CRF}$$

2. Capital recovery factor

The capital recovery factor (CRF), which converts the total CAPEX into uniform annual payments over the project lifetime, was applied. The discount rate i was set to 10%, and the CRF was determined using the following equation:

$$\text{Capital recovery factor} = \frac{i(1+i)^n}{(1+i)^n - 1}$$

where n is the project lifetime in years.

3. The capacity factor is assumed to be 0.8, indicating that the plant does not operate continuously but functions at 80% of its full-time capacity[1].

4. CAPEX estimation

The CAPEX was estimated from a 2016 study[2] using a scaling factor n of 0.6. The values were then adjusted to reflect 2023 economic conditions based on the Chemical Engineering Plant Cost Index (CEPCI). It was calculated as follows:

$$\text{Cost}_{2023} = \text{Cost}_{2016} \left(\frac{\text{Capacity}_{2023}}{\text{Capacity}_{2016}}\right)^n \left(\frac{\text{CEPCI}_{2023}}{\text{CEPCI}_{2016}}\right)$$

5. Electrolyzer Cost Estimation[1]

Based on the total required current and an assumed operating current density of 125 mA/cm², the necessary electrolyzer area can be calculated using the following equation:

$$\text{Area of electrolyzer} = \frac{I}{i} (\text{m}^2)$$

where I is the total current and i is the current density.

The capital cost of the electrolyzer is then estimated using a unit cost of \$10,000 per m²:

$$\text{Cost of electrolyzer} = \text{Area of electrolyzer} \times \$10{,}000/\text{m}^2$$

In addition, the combined cost of the catalyst and membrane is assumed to be 5% of the electrolyzer cost:

$$\text{Catalyst and membrane cost} = \text{Cost of electrolyzer} \times 0.05$$

6. Both operating and maintenance costs are assumed to account for 10% of the capital expenditure[1].

7. A DMSO recovery rate of 99.9% is assumed, with the remaining 0.1% replenished through makeup.

8. The recovery of PMA and H_2SO_4 is assumed to be 99.9%.

9. The reactor operates at 100 °C, while the electrolyzer is maintained at 25 °C. The separation step at 180 °C is employed to recover and recycle PMA, H_2SO_4, and DMSO from the aqueous FA mixture. The utility cost includes the costs of heat supply and electricity, assuming ideal heat exchange.

10. Formic acid Distillation

The CAPEX and OPEX required for the distillation of formic acid were estimated by fitting data from the study by Laitinen et al. (2021) using a power-law model. In this study, the concentration of FA was 0.835 wt%.

11. Minimum selling price (MSP) of TPA calculation

The MSP of TPA is the break-even product price at which the total annualized cost of the process equals the annual revenue. Accordingly, the MSP is calculated by dividing the total annual cost by the annual TPA production:

$$\mathrm{MSP} = \frac{\text{Total annual cost}}{\text{Annual TPA production}}$$

Table S5. CAPEX and OPEX for formic acid (FA) distillation at varying FA concentrations.

FA concentration(wt%)	CAPEX ($/kg FA)	OPEX ($/kg FA)	Reference
5	0.066	0.316	5
10	0.056	0.189	5
20	0.052	0.141	5
0.835	0.0884	0.863	This study

Supporting References

1. H. Zhou, Y. Ren, Z. Li, M. Xu, Y. Wang, R. Ge, X. Kong, L. Zheng and H. Duan, Nature Communications, 2021, 12, 4679.
2. R. B. C. W. W. B. J. S. A. R. T. D. Bhattacharyya, Analysis, Synthesis, and Design of Chemical Processes, Fifth Edition, Prentice Hall, 2018.
3. H. Junghare, M. Hamjade, C. K. Patil, S. B. Girase and M. M. Lele, International Journal of Current Engineering and Technology, 2017, 7, 420-423.
4. A. Singh, N. A. Rorrer, S. R. Nicholson, E. Erickson, J. S. DesVeaux, A. F. T. Avelino, P. Lamers, A. Bhatt, Y. Zhang, G. Avery, L. Tao, A. R. Pickford, A. C. Carpenter, J. E. McGeehan and G. T. Beckham, Joule, 2021, 5, 2479-2503.
5. A. T. Laitinen, V. M. Parsana, O. Jauhiainen, M. Huotari, L. J. P. van den Broeke, W. de Jong, T. J. H. Vlugt and M. Ramdin, Industrial & Engineering Chemistry Research, 2021, 60, 5588-5599.